



Sustainable potable water production using a solar still with photovoltaic modules-AC heater

Ali Riahi^{a,*}, Khamaruzaman Wan Yusof^a, Balbir Singh Mahinder Singh^b,
Mohamed Hasnain Isa^a, Emmanuel Olisa^a, Noor Atieya Munni Zahari^a

^aDepartment of Civil and Environmental Engineering, Universiti Teknologi PETRONAS, 32610 Bandar Seri Iskandar, Perak, Malaysia, emails: ali_riahiupm@yahoo.com (A. Riahi), khamaruzaman.yusof@petronas.com.my (K. Wan Yusof), hasnain@petronas.com.my (M.H. Isa), emidear2003@yahoo.com (E. Olisa), tieymunn@yahoo.com (N.A.M. Zahari)

^bDepartment of Fundamental and Applied Sciences, Universiti Teknologi PETRONAS, 32610 Bandar Seri Iskandar, Perak, Malaysia, email: balbir@petronas.com.my

Received 6 October 2014; Accepted 2 July 2015

ABSTRACT

Solar energy as a sustainable energy source can be harnessed to produce potable water using solar stills. In this work, effort was made to evaluate the performance of a double slope solar still integrated with a 500 W heater to produce potable water. The heater was powered by six photovoltaic modules, which can produce 1.5 KWp and then connected to four batteries with capacity of 150 Ah each. The experiments were conducted over several days in the tropical climate of Malaysia. A black painted steel trough with length 90 cm, width 45 cm, and depth 8 cm was used as the basin of the glass covered double slope solar still. A comparison of the cumulative water production between the conventional solar still (CSS) and solar still with PV-Heater (CSSPVH) was done. The CSSPVH was found to be more effective; producing about six times the amount of water produced by the CSS. Mathematical models derived based on energy balance studies of CSSPVH, were used to carry out simulations to verify the experimental findings. The energy balance equations of condensing cover and the basin water of CSSPVH were developed as well. A good agreement was found between numerical and experimental productivities of CSSPVH. An expected increase in water production of up to 16 kg/m² per 24 h was obtained using CSSPVH. Therefore, CSSPVH is an effective design to produce sustainable potable water, even in areas with very low daily solar radiation intensity, due to its ability to store solar energy. In addition, some tested water quality parameters indicate that water produced from solar stills meet the WHO standard for potable water.

Keywords: Solar energy; Heat and mass transfer; Photovoltaic module; Solar still; Water heater

1. Introduction

Solar distillation still is a fundamental technique for producing healthy and safe drinking water by

removing the heavy metals and chemicals from groundwater and seawater [1,2] in arid, remote, and coastal areas. These areas have plenty of solar energy. In current years, researchers have carried out theoretical and experimental attempts on active solar stills performance with the use of external heat energy

*Corresponding author.

source as well as available solar radiation intensity to enhance the basin water temperature and solar still productivity. A double slope active solar still coupled with photovoltaic thermal (PVT) was designed and fabricated in India [3]. A DC water pump connected to the photovoltaic module was operated to circulate the preheated water flow between solar collectors and the solar still. A higher experimental productivity of $3.77 \text{ kg/m}^2 \text{ d}$ was obtained as compared to the water production of $2.69 \text{ kg/m}^2 \text{ d}$ for the single slope hybrid (PVT) solar still. A thermal analysis of a single slope solar still coupled with optimum number of evacuated tube collector was developed in India [4]. The daily energy and exergy efficiencies of up to 33.05 and 2.5% with the highest output of $3.8 \text{ kg/m}^2 \text{ d}$ were observed with a combination of 10 evacuated tubes and water depth of 0.03 m in the basin.

A comparative study of the performance of an inverted absorber solar still (IASS) and a single slope solar still (SS) conducted in Muscat, Oman [5], found that the IASS enhanced the experimental water production by 192% with a maximum capacity of $6.3 \text{ L/m}^2 \text{ d}$. A theoretical analysis of IASS was carried out to evaluate its water production performance, where 5.1, 4.8, and $4.5 \text{ kg/m}^2 \text{ d}$ at water depths of 0.01, 0.02, and 0.03 m, respectively, were produced [6].

A solar still using a parabolic-trough concentrator was fabricated with thermal insulation and wind protection in Cocayalta, Peru [7]. Its productivity was $6.36 \text{ L/m}^2 \text{ d}$ compared to $3.25 \text{ L/m}^2 \text{ d}$ for a model without insulation.

In Saudi Arabia, two water heaters each with maximum power output of 500 W and one electrically powered cooling fan were used, and their effects were investigated theoretically and experimentally to improve water production of a double slope solar still [8]. The insulation of water heater increased the experimental productivity to $11.8 \text{ L/m}^2 \text{ d}$ as compared to $2.5 \text{ L/m}^2 \text{ d}$ obtained from the conventional still without the heater. A development of energy balance equations for the condensing cover, basin and water were obtained, respectively, for the solar still using mathematical modeling. A close agreement between the numerical and experimental results was achieved and the use of water heaters powered by PV modules to reduce cost was suggested.

A comprehensive review of literature shows that the use of an active solar still integrated with a 500 W AC heater powered by six monocrystalline photovoltaic modules (each with maximum capacity of 245 W) and connected to four batteries (each with capacity of 150 Ah each) as an application of external heat energy source to improve the still productivity has not been reported (CSSPVH). Previous studies

[3,4,7,9–14] showed a sharp decline in water production after 2 pm due to decline in solar radiation. The conventional solar still (CSS) and active and passive solar stills cannot produce steady amount of water once there is a reduction in solar radiation. But the CSSPVH reported in this work, has the ability to maintain a constant production of water in terms of the amount being produced even when there is no solar radiation; due to the integration of the solar power system. Therefore, room still exists for further enhancement of the performance of solar still via innovative designs and configurations. Thus, the main objective of this work is to investigate the productivity enhancement of a solar still integrated with PV-powered AC heater compared to the conventional type. Mathematical models of CSSPVH was also simulated using the relations of heat and mass transfer to develop the energy balance equations of condensing glass cover and basin water. The numerical and experimental productivities of CSSPVH were also compared.

2. Mathematical modeling

Fig. 1 shows the energy balance diagram of double slope solar still combined with PV-AC heater. A mathematical model was developed for the use of photovoltaic module, batteries, and alternating current (AC) water heater.

The equation for conservation of mass is given by Malik et al. [15].

$$M_{\text{in}} = m_{\text{fw}} - m_{\text{bd}} \quad (1)$$

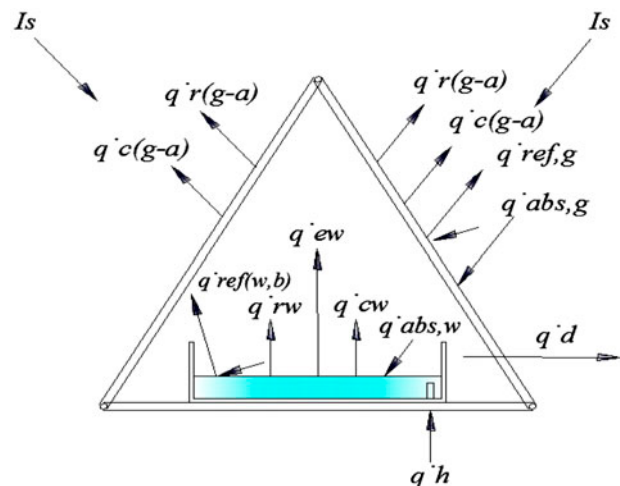


Fig. 1. Schematic diagram of heat transfer process in CSSPVH.

The energy balances (in W) for condensing cover, basin, and water are as follows:

The energy balance equation of condensing glass cover (dE_g/dt) is written as Eqs. (2) and (3) [16].

$$(dE_g/dt) = \dot{q}_{abs,g} + \dot{q}_{ew} + \dot{q}_{cw} + \dot{q}_{rw} - \dot{q}_{c(g-a)} - \dot{q}_{r(g-a)} - \dot{q}_{ref(g-a)} \quad (2)$$

$$(dE_g/dt) = m_g C_g (dT_g/dt) \quad (3)$$

The energy balance equation for basin and water ($dE_{w,b}/dt$) using additional external heat energy source of a 500 W AC heater is written as Eqs. (4) and (5).

$$(dE_{w,b}/dt) = \dot{q}_{abs,w} + \dot{q}_{heater} - \dot{q}_{ew} - \dot{q}_{cw} - \dot{q}_{rw} - \dot{q}_{ref(w,b)} - \dot{q}_d \quad (4)$$

$$(dE_{w,b}/dt) = (m_w C_w + m_b C_b) (dT_w/dt) \quad (5)$$

The following assumptions were made to solve the energy balance equations.

- (1) T_g is uniform over the glass surface based on the experimental data.
- (2) T_w is uniform over the basin water and was obtained from experimental data.
- (3) $\dot{q}_{ref(w,b)}$ and $\dot{q}_{ref(g-a)}$ which are the heat reflected from water surface and glass cover to atmosphere, are negligible.

The hourly condensed water production rate per unit area (M_{hn}) is calculated by [6]:

$$M_{hn} = (\dot{q}_{ew}/L) \times 3,600 \text{ kg/m}^2 \text{ h} \quad (6)$$

The rates of convective, radiative, and evaporative heat transfer (\dot{q}_{cw} , \dot{q}_{rw} , and \dot{q}_{ew}) from water surface to the cover are expressed, respectively, as the following equations [15]:

$$\dot{q}_{cw} = h_{cw} A_b (T_w - T_g) \quad (7)$$

$$\dot{q}_{rw} = h_{rw} A_b (T_w - T_g) \quad (8)$$

$$\dot{q}_{ew} = h_{ew} A_b (T_w - T_g) \quad (9)$$

The convective, radiative, and evaporative heat transfer coefficients from water to condensing cover (h_{cw} , h_{rw} , and h_{ew}) are calculated as follow [6]:

$$h_{cw}: 0.884 [T_w - T_g + (P_w - P_g) \times (T_w + 273)/268.9 \times 10^3 - P_w]^{1/3} \quad (10)$$

$$h_{rw} = \epsilon_{eff} \sigma [(T_w + 273)^2 + (T_g + 273)^2] \times [T_w + T_g + 546] \quad (11)$$

$$\epsilon_{eff} = [1/\epsilon_g + 1/\epsilon_w - 1]^{-1} \quad (12)$$

$$h_{cw}: 16.273 \times 10^{-3} h_{cw} (P_w - P_g) / (T_w - T_g) \quad (13)$$

The parameter ϵ_{eff} is the effective emissivity. The saturated vapor pressure at basin water temperature and condensing glass cover surface (P_w and P_g) can be obtained according to Toure and Meukam [17] as follows:

$$P_w = 7235 - 431.45T_w + 10.76T_w^2 \quad (14)$$

$$P_g = 7235 - 431.45T_g + 10.76T_g^2 \quad (15)$$

The rate of heat transfer of solar radiation absorption by condensing glass cover ($\dot{q}_{abs,g}$) is given by Murugavel et al. [18]:

$$\dot{q}_{abs,g} = \alpha_g A_{g,E} I_E + \alpha_g A_{g,W} I_w \quad (16)$$

The rate of heat transfer of solar radiation absorption by basin water due to passing solar radiation from glass cover ($\dot{q}_{abs,w}$) is reported by Murugavel et al. [18]:

$$\dot{q}_{abs,w} = \alpha_w A_{g,E} \tau_g I_E + \alpha_w A_{g,W} \tau_g I_w \quad (17)$$

The amount of output power of PV module exposed to direct solar radiation ($P_{output,pv}$) is calculated using Eq. (18) suggested by Herrando et al. [19]. The maximum rate of power capacity of the AC heater is 500 W, which receives power directly from batteries.

$$P_{output,pv} = n \times \eta_{pv} \times A_{pv} \times I_s \quad (18)$$

The rate of convective and radiative heat losses from condensing glass cover to the ambient air ($\dot{q}_{c(g-a)}$ and $\dot{q}_{r(g-a)}$) are as follows [15]:

$$\dot{q}_{c(g-a)} = h_{c(g-a)} A_g (T_g - T_a) \quad (19)$$

$$\dot{q}_{r(g-a)} = \sigma \epsilon_g A_g (T_g^4 - T_a^4) \quad (20)$$

According to Watmuff et al. [20], the convective heat transfer coefficient from cover to ambient air ($h_{c(g-a)}$) can be calculated by Eq. (21).

$$h_{c(g-a)} = 5.7 + 3.8V \quad (21)$$

The heat loss from solar still due to evaporation from the system (\dot{q}_d) [15] is:

$$\dot{q}_d = m_d C_w (T_w - T_a) \quad (22)$$

The constants used in these numerical calculations are:

$$A_g = 1.2 \text{ m}^2, \quad A_b = 0.405 \text{ m}^2, \quad C_b = 452 \text{ J/kg K}, \\ C_w = 4,178 \text{ J/kg K}, \quad \tau_g = 0.835, \quad \alpha_g = 0.127, \quad \alpha_s = 0.69, \\ \varepsilon_g = 0.9, \quad m_w = 15 \text{ kg}, \quad m_b = 10 \text{ kg}, \quad m_g = 8 \text{ kg}, \quad C_g = \\ 840 \text{ J/kg K}, \text{ and } \varepsilon_{wg} = 0.9.$$

3. Experimental setup

Figs. 2 and 3 show the schematic diagram and photograph of the five stages of the experimental setup of the solar stills. Water from a lake in Universiti Teknologi PETRONAS (UTP) was collected to feed the solar still basin (Fig. 3(a)). A water tank was used to feed 15 L of lake water into the solar still basin up to a depth of 4 cm. The 4 cm depth was maintained throughout the experiment by constantly refilling lake water into the solar still basin (Fig. 3(b)).

A single basin double slope solar still (conventional solar still) was constructed with a steel trough as the still basin having a length of 90 cm, width of 45 cm, and depth of 8 cm (volume 32.4 L). A double slope glass cover with a tilt angle of 60°, length of 100 cm, and width of 60 cm was fabricated for this solar still (Fig. 3(b)). An aluminum sheet connected to two funnels embedded at the two side holes of the basin were used to collect the water vapor that condensed on the four sides of the glass covers.

The solar power system in this work consisted of a 500 W alternating current (AC) water heater, which was electrically powered by six monocrystalline PV modules with peak power output of 245 W each. Each PV module had an area of 1.6 m × 0.96 m (1.536 m²) (Figs. 2 and 3(e)). The maximum power output from these six PV modules was 1,470 W. The power of the PV modules was regulated using a 30A charge regulator (Fig. 3(e)). A total of 4 × 12 V batteries each with capacity of 150 Ah were charged by the six PV modules (Fig. 3(d) and (e)). The batteries were connected in series to each other. The DC power from the batteries was converted to AC power by the use of a 2 kW inverter, enough to supply electricity to the heater

(Fig. 3(e)). The schematic diagram of this system is shown in Fig. 2.

The two types of solar stills studied were:

Solar still 1 (CSS)—Conventional solar still is shown in Fig. 3(b).

Solar still 2 (CSSPVH)—Conventional solar still integrated with a 500 W AC heater was connected to 4 × 150 Ah batteries and 6 × 245 W photovoltaic modules is shown in Fig. 3(c)–(e).

Experiments were conducted for 6 d on 18 February 2014, 24 March 2014, 10 April 2014, 07 May 2014, 17 May 2014, and 14 June 2014 in a solar field in Universiti Teknologi PETRONAS campus in Malaysia to investigate the performance of these solar stills.

Experiment 1—Solar still 1 (CSS) was exposed to available solar radiation in an open field (Solar field) for three days on 07 May 2014, 17 May 2014, and 14 June 2014.

Experiment 2—Solar still 2 (CSSPVH) was exposed to available solar radiation at the same location as Experiment 1 for three different days on 18 February 2014, 24 March 2014, and 10 April 2014.

Temperatures of water, inner cover of solar stills and ambient air were measured hourly using a digital thermocouple. Solar radiation intensity was measured at time interval of 5 min using a pyranometer. The volume of condensed water collected was measured hourly using a measuring cylinder. Hourly wind speed was also measured using an anemometer. The accuracy and measurement range of the instruments used are shown in Table 1.

The specifications of alternating current (AC) water heater, solar charge regulator, PV modules, and batteries used in the experiments are shown in Table 2.

4. Results and discussion

4.1. Observations of overall findings of CSS and CSSPVH

Table 3 shows the average solar radiation intensities, average water temperatures, cumulative experimental productivity of CSS, and cumulative experimental and numerical water production of CSSPVH during the experimental days. Experiments were conducted for three days for each solar still from 9 am to 5 pm.

It was observed that with the increase in average solar radiation intensities, average water temperature, and cumulative productivities increased, respectively, for both solar stills (Table 3). It showed that the highest average solar radiation intensity occurred on 24 March 2014 with the value of 823 W/m², which caused the average water temperature and cumulative experimental productivity to reach the highest value

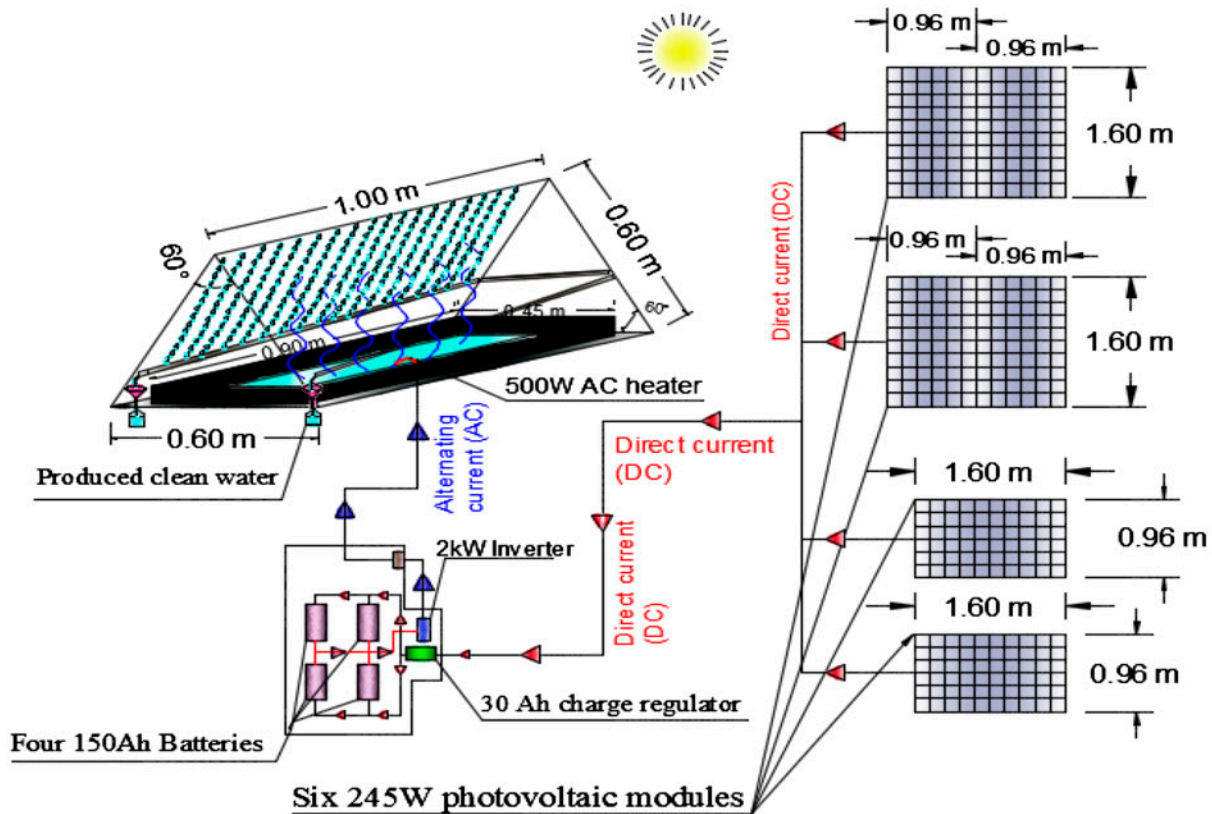


Fig. 2. Schematic diagram of CSSPVH.

Table 1
Experimental instruments with accuracy and range

Instruments	Accuracy	Range
Digital thermocouple	±1 °C	0–100 °C
Pyranometer	±1 W/m ²	0–3,000 W/m ²
Measuring cylinder	±0.5 ml	0–50 ml
Anemometer	±0.1 m/s	0.2–30 m/s

of 57 °C and 5.7 kg/m², respectively, for CSSPVH, with the aid of external energy source of PV-AC heater.

Results in Table 3 also show that the values of average water temperature and cumulative experimental productivity for CSSPVH were always higher than the corresponding values for CSS.

Table 2
Specifications of AC water heater, solar charge regulator, photovoltaic modules, and batteries used in this work

Parameters	AC water heater	Solar charge regulator	Photovoltaic modules	Batteries
Maximum power voltage (V_{pmax})	220 V	24 V	30.1 V	12 V
Maximum power output (P_{max})	500 W	720 W	245 W	1,800 Wh
Maximum current power (I_{pmax})	2.27 A	30 A	8.23 A	150 Ah
Open circuit voltage (V_{oc})	NA	NA	37.1 V	NA
Short circuit current (I_{sc})	NA	NA	8.80 A	NA

The cumulative experimental productivity for CSSPVH reached the highest value of 5.7 kg/m² with the average T_w of 57.33 °C and average I_s of 823 W/m² on 24 March 2014 as a result of the additional external energy source of integration with PV modules, solar batteries, and alternating current heater as well as available solar radiation intensity, while the highest obtained cumulative productivity for CSS was 0.9 kg/m² with the average T_w of 47.11 °C and average I_s of 778 W/m² on 07 May 2014 with only use of the accessible solar radiation intensity. It is concluded that the highest cumulative productivity for CSSPVH is almost six times higher than the highest water produced by CSS.

Figs. 4 and 5 show the variations of solar radiation intensity for three different typical days for CSSPVH

Table 3

Average of solar radiation intensity, average water temperature, experimental, and numerical cumulative productivity of CSS and CSSPVH from 9 am to 5 pm during experimental days

Date	Solar still	Average I_s (W/m ²)	Average T_w (°C)	Cumulative experimental productivity (M_{cexp}) (kg/m ²)	Cumulative numerical productivity (M_{cn}) (kg/m ²)
18 February 2014	CSSPVH	727	57.22	5.3	5.5
24 March 2014	CSSPVH	823	57.33	5.7	5.8
10 April 2014	CSSPVH	650	57.11	5.1	5.2
07 May 2014	CSS	778	47.11	0.9	NA
17 May 2014	CSS	563	41.33	0.6	NA
14 June 2014	CSS	559	41.56	0.6	NA

and CSS from 9 am to 5 pm with measured time interval of 5 min using a Pyranometer. Fig. 6 shows the variations of hourly output power of six PV modules transferred to the four batteries to charge and to power the AC heater inside the basin of the double slope solar still from 9 am to 5 pm. It is observed that with the increase in radiation intensities from 9 am to about 2 pm for three days, which are; 18 February 2014, 24 March 2014, and 10 April 2014, the water temperature of CSSPVH increased to the highest values due to the aid of the output power of the heater ($P_{output,heater}$) used in CSSPVH (Figs. 6 and 7).

However, the water temperature of CSS on 07 May 2014 and 14 June 2014 reached the highest values from 9 am to 1 pm with the increase in only available solar intensities. While it is observed that the obtained highest values of T_w for CSSPVH was clearly higher than those values for CSS due to the aid of output power of the heater ($P_{output,heater}$) used in the solar still (Figs. 6–8).

4.2. Effect of solar radiation intensity on performance of CSSPVH and CSS

Two typical days with the range of solar radiation intensity from 700 to 800 W/m² were selected to evaluate the numerical and experimental results obtained from CSSPVH and to compare them with the experimental results of CSS. On the first day (18 February 2014), the experiment was conducted using CSSPVH, with the average solar radiation intensity of 727 W/m² and on the second day (07 May 2014) the experiment was conducted using CSS, with the average solar radiation intensity of 778 W/m². Both days were discretely selected because the average solar radiation intensity falls within the same range, when compared to that of the other experimental days (Table 3).

Fig. 9 shows the variations of solar radiation intensities (I_s), rates of heat energy transfer of glass cover

absorption of CSSPVH ($\dot{q}_{abs,g}$), basin water absorption of CSSPVH ($\dot{q}_{abs,w}$), rate of output power of six photovoltaic modules ($P_{output,pv}$) with time interval of 5 min and the rate of maximum output power of AC heater ($P_{output,heater}$) from 9 am to 5 pm on a typical day (18 February 2014). The diurnal variations of temperatures of water, inner glass of CSSPVH and ambient temperature vs. the rate of evaporative (\dot{q}_{ew}), convective (\dot{q}_{cw}), and radiative (\dot{q}_{rw}) heat energy transfer of CSSPVH from 9 am to 5 pm on that day are shown in Fig. 10. The highest $\dot{q}_{abs,g}$, $\dot{q}_{abs,w}$, $P_{output,pv}$, T_w , T_g , T_a , \dot{q}_{ew} , \dot{q}_{cw} , and \dot{q}_{rw} of 199.1 W, 903.28 W, 1,470 W, 65°C, 52°C, 32°C, 190.05 W, 33.38 W, and 14.11 W were observed, respectively, when I_s peaked at 1038.27 W/m² at about 2:30 pm (Figs. 9 and 10). With the aid of an external output battery power, the output power of the heater remained constant at 500 W between 9 am and 5 pm. With decrease in I_s to 200 W/m² at 5 pm from its highest value at 2:30 pm, the values of $\dot{q}_{abs,g}$, $\dot{q}_{abs,w}$, $P_{output,pv}$, and T_a decreased sharply due to their sole dependency on I_s (Eqs. (16)–(18)), while the values of T_w , T_g , \dot{q}_{ew} , \dot{q}_{rw} , and \dot{q}_{cw} reduced slightly due to the external power and energy received from the heater and batteries. There are some instant fluctuations of solar radiation intensities from 9 am to 5 pm which caused instant decrease in the values of $\dot{q}_{abs,g}$, $\dot{q}_{abs,w}$, $P_{output,pv}$ (Fig. 9).

The wind speed (V) and the rate of convective heat losses from the condensing glass cover of CSSPVH to the atmosphere ($\dot{q}_{c(g-a)}$) are shown in Fig. 11. It is observed that with the decrease in wind speed from 9 am to 1 pm the rate of $\dot{q}_{c(g-a)}$ increased due to the sharp increase in inner glass and ambient temperature differences (Fig. 10, Eqs. (19) and (21)). During the rest of the day from 1 pm to 5 pm the $\dot{q}_{c(g-a)}$ increased due to a corresponding increase in wind speed.

The variations in temperature of water, inner glass of CSS and ambient temperature on 07 May 2014 from 9 am to 5 pm are shown in Fig. 12. It was observed that

T_w and T_g increased gradually to the peak values of 50°C and 44°C, respectively, with the increase in solar radiation intensity from 399.78 W/m² at 9 am to 859.99 W/m² at 2 pm (Figs. 5 and 12); thereafter they decreased with the reduction of solar radiation intensity from 2 pm to 5 pm. These results were observed to be similar to the findings of other researchers [10–14].

4.3. Hourly and cumulative water production of CSS and CSSPVH

Figs. 13 and 14 show the experimental and numerical productivities of CSSPVH and the experimental water production of CSS on 18 February 2014 and 07 May 2014, respectively. It was observed that with the similar average solar radiation intensity during the two experimental days of 18 February 2014 and 07 May 2014 (Table 3, Figs. 4 and 5) and similar volume of initial feed water (15 L) in the basins of the CSS and CSSPVH, the average water and inner glass temperatures, and hourly and cumulative water production of CSSPVH showed markedly higher values as compared to the corresponding average T_w , T_g , M_{hexp} , and M_{cexp} of CSS (Table 3, Figs. 10, 12–14). These differences occurred as a result of the additional 500 W AC heater that was used as an external heat energy source connected to 6 × 245 W photovoltaic modules and 4 × 150 Ah batteries to the CSSPVH basin (Figs. 2 and 3).

The hourly experimental water production (M_{hexp}) from CSS and CSSPVH peaked to 0.2 and 0.8 kg/m², respectively, at about 2 pm (Figs. 13 and 14). M_{hexp} of CSSPVH was about four times that of CSS. The water temperature and hourly water production of this active solar still (CSSPVH) showed almost similar values from 2 pm to 5 pm with the aid of external heat energy source of PV modules, batteries and AC heater even though there is a decrease in solar radiation intensity during this period of time (Fig. 13). While, the water temperature and hourly output showed a sharp decrease for CSS and also other passive and active solar stills with the decrease in solar radiation intensity from 2 pm onward [3,4,7,9–14].

The experimental cumulative water production from both solar stills showed a clear difference in productivity due to use of the solar power system. CSSPVH also had a higher experimental cumulative productivity (M_{cexp}) of 5.3 kg/m² as compared to the corresponding productivity of 0.9 kg/m² for CSS. It shows that M_{cexp} of CSSPVH was about six times higher that of CSS (Figs. 13 and 14). Fig. 13 also shows the values of experimental and numerical hourly and cumulative productivities of CSSPVH on 18 February 2014. The experimental and numerical cumulative productivities

of CSSPVH were 5.3 and 5.5 kg/m², respectively, on 18 February 2014 (Fig. 13). Both hourly and cumulative productivities showed good agreement between the experimental and numerical values.

The relationship of numerical and experimental hourly production (M_{hn} , M_{hexp}) with the rate of evaporative heat energy transfer (\dot{q}_{ew}) of CSSPVH is shown in Figs. 15 and 16, respectively. The value of R^2 should be exactly equal to 1, from the use of the mathematical Eq. (6), which is used to determine the numerical hourly productivity of CSSPVH. However, the relationship between experimental hourly water production (M_{hexp}) and the rate of evaporative heat energy transfer (\dot{q}_{ew}) was equal to 0.9865, which is close to the value of R^2 and also shows the linear relationship between M_{hexp} and \dot{q}_{ew} as well. It is deduced that the numerical hourly and cumulative productivities of CSSPVH correlate well with the experimental values.

4.4. Heat energy balance of CSSPVH

The heat energy values for condensing cover and basin water of CSSPVH from 9 am to 5 pm on 18 February 2014 are shown in Tables 4 and 5, respectively. Table 4 shows that the rate of heat energy absorption of solar radiation intensity by the condensing glass cover ($\dot{q}_{\text{abs,g}}$) and the rates of convective and radiative heat losses from it to the ambient air ($\dot{q}_{\text{c(g-a)}}$ and $\dot{q}_{\text{r(g-a)}}$) (–1583.10 W) is almost equal to the rate of mass transfer from glass cover ($m_g C_g (dT_g/dt)$) minus the cumulative evaporative (\dot{q}_{ew}), convective (\dot{q}_{cw}), and radiative (\dot{q}_{rw}) rate of heat energy transfer of basin and water, respectively (–1549.26 W).

Likewise, it was observed (Table 5) that the rate of heat energy absorption of solar radiation intensity by the basin water ($\dot{q}_{\text{abs,w}}$) and the additional rate of heat energy from AC heater (\dot{q}_h) (6503.40 W) is almost equal to the rate of mass transfer of water and basin ($(m_w C_w + m_b C_b) (dT_w/dt)$) plus the cumulative rate of heat energy transfer of evaporative (\dot{q}_{ew}), convective (\dot{q}_{cw}), and radiative (\dot{q}_{rw}) plus the rates of heat losses from distilled water to the ambient air (\dot{q}_d) (6569.42 W).

4.5. Evaluation of output power storage in batteries using pv modules

Table 6 shows the hourly solar radiation intensity (I_s), hourly output power of six photovoltaic modules ($P_{h,pv}$), and cumulative output power of six photovoltaic modules stored in batteries ($P_{c,pv}$) on 18 February 2014 from 7 am to 7 pm. Cumulative solar

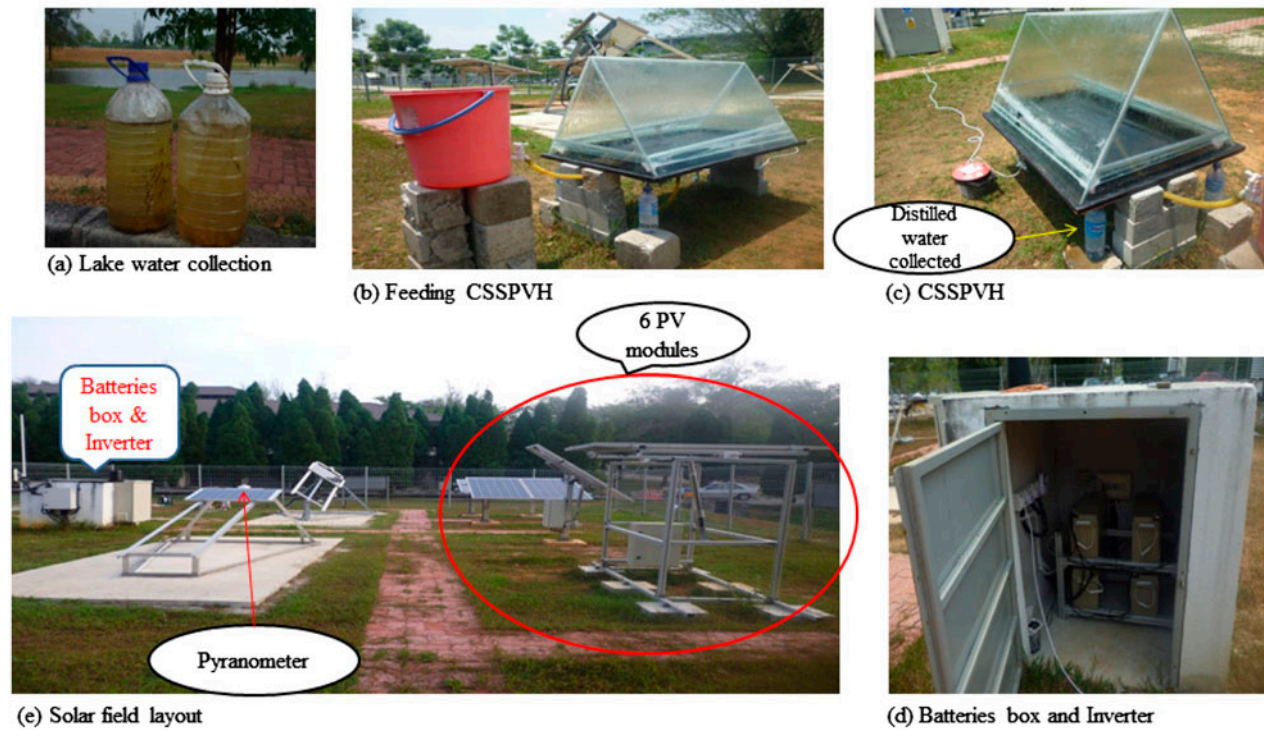


Fig. 3. Photograph of experimental setup.

Table 4

Heat energy values of condensing glass cover of CSSPVH (Eqs. (2) and (3)) on 18 February 2014 from 9 am to 5 pm

Time (h)	$\dot{q}_{\text{abs},g} - \dot{q}_{c(g-a)} - \dot{q}_{r(g-a)}$ (W)	=	$m_g C_g (dT_g/dt)$ (W)	-	$\dot{q}_{\text{ew}} + \dot{q}_{\text{cw}} + \dot{q}_{\text{rw}}$ (W)
9 am	20.51		46.67		2.96
10 am	-153.41		5.60		67.57
11 am	-139.27		1.87		161.40
12 pm	-150.81		7.47		205.58
1 pm	-115.59		3.73		231.14
2 pm	-188.93		-3.73		237.55
3 pm	-289.97		-3.73		237.55
4 pm	-196.09		-3.73		231.14
5 pm	-369.53		-3.73		224.79
Cumulative	-1583.10	=	50.40	-	1599.66
Total heat energy (W)	-1583.10		-1549.26		

intensities for every 5 min per hour divided by 12 is equal to hourly solar radiation intensity (I_s) is shown in Fig. 4 and Table 6. The maximum power voltages of four batteries (V_{pmax}) are 4×12 V (Table 2). The four batteries were connected in series. Then the maximum power voltages of four batteries (V_{pmax}) were converted from 4×12 V to 2×24 V. The maximum hourly power capacity ($P_{\text{max,batteries}}$) of four batteries was calculated as $150\text{Ah} \times 24 \text{V} \times 2$ (7,200 W h). One AC heater with the maximum power output ($P_{\text{max,heater}}$)

of 500 W was used in the experiment from 9 am to 5 pm (Table 2). The hourly output power of six PV modules in Table 6 ($P_{h,\text{pv}}$) was calculated by taking the average output power of the PV modules in every 5 min during each hour in Figs. 6 and 9. Values of $P_{c,\text{pv}}$ were calculated by accumulating the values of $P_{h,\text{pv}}$ from 7 am to 7 pm (Figs. 6, 9 and Table 6).

Table 6 also shows that when solar intensity increased to 354.16W/m^2 from 9 am to 10 am, the AC heater can be used due to the charging of the batteries

Table 5

Heat energy values of basin water of CSSPVH (Eqs. (4) and (5)) on 18 February 2014 from 9 am to 5 pm

Time (h)	$\dot{q}_{abs,w}$ (W)	+ \dot{q}_h (W)	= $(m_w C_w + m_b C_b) (dT_w/dt)$ (W)	+ $\dot{q}_{ew} + \dot{q}_{ew} + \dot{q}_{rw}$ (W)	+ \dot{q}_d (W)
9 am	105.06	500.00	485.26	2.96	34.82
10 am	211.92	500.00	205.30	67.57	379.46
11 am	316.98	500.00	55.99	161.40	504.98
12 pm	397.69	500.00	74.66	205.58	513.65
1 pm	425.65	500.00	55.99	231.14	543.95
2 pm	450.00	500.00	-18.66	237.55	543.84
3 pm	151.05	500.00	-18.66	237.55	543.07
4 pm	378.31	500.00	-18.66	231.14	527.17
5 pm	66.73	0.00	-37.33	224.79	594.95
Cumulative	2503.40	+ 4000.00	= 783.88	+ 1599.66	+ 4185.88
Total heat energy (W)	6503.40		6569.42		

Table 6

Hourly and cumulative output power of six photovoltaic modules stored in batteries^a

Time	I_s (W/m ²)	$P_{h,pv}$ (Wh)	$P_{c,pv}$ (W)
7 am–8 am	13.3	10.21	10.21
8 am–9 am	131.57	242.51	252.72
9 am–10 am	354.16	652.80	905.52
10 am–11 am	570.45	1051.47	1956.99
11 am–12 pm	793.47	1434.37	3391.36
12 pm–1 pm	904.48	1,470	4861.36
1 pm–2 pm	933.83	1415.44	6276.8
2 pm–3 pm	939.12	1428.67	7705.47
3 pm–4 pm	816.13	1369.18	9074.65
4 pm–5 pm	506.16	870.34	9944.99
5 pm–6 pm	331.48	610.99	10555.98
6 pm–7 pm	231.09	394.93	10950.91

Notes: $P_{c,pv}$: cumulative output power of six photovoltaic modules stored in batteries.

^a $P_{h,pv}$: hourly output power of six photovoltaic modules stored in batteries.

with the cumulative output power from the six PV modules. With the increase in I_s from 354.16 W/m² at 10 am to 939.12 W/m² at 3 pm the values of $P_{h,pv}$ and $P_{c,pv}$ increased as well. When the average hourly solar radiation intensity reached 904.48 W/m² from 12 pm to 1 pm without showing any fluctuations (Figs. 6 and 9), the output power of six PV modules peaked at the highest value of 1,470 W h. With the decrease in I_s from 4 pm to 7 pm the values of $P_{h,pv}$ decreased as well (Table 6). The overall cumulative output power of PV modules ($P_{c,pv}$) was found to be 10950.91 W during the accessibility of solar radiation intensity from 7 am to 7 pm (Table 6). The rates of output power of six PV-modules ($P_{output,pv}$) and the rate of maximum output power of one 500 W AC heater

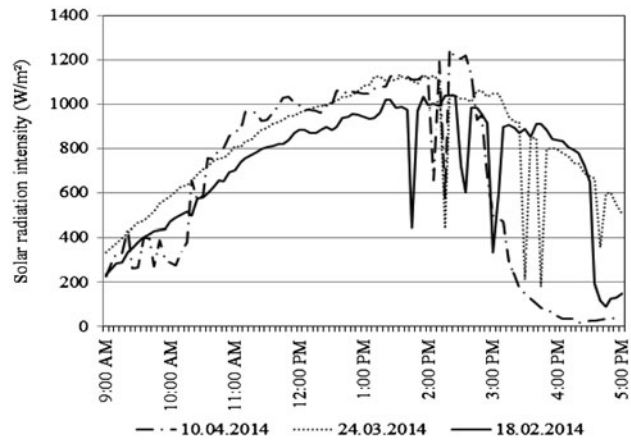


Fig. 4. Solar radiation intensity for three typical days from 9 am to 5 pm using CSSPVH.

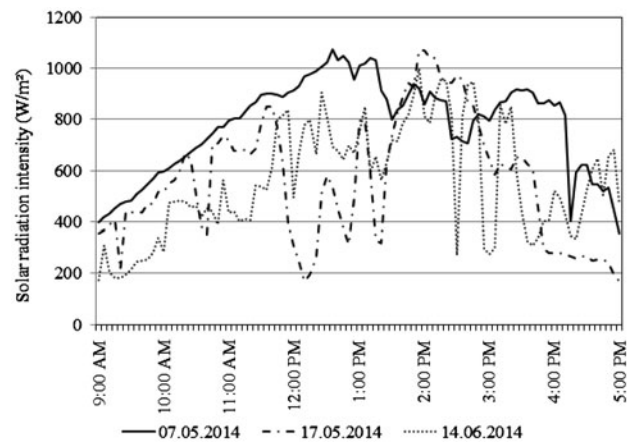


Fig. 5. Solar radiation intensity for three typical days from 9 am to 5 pm using CSS.

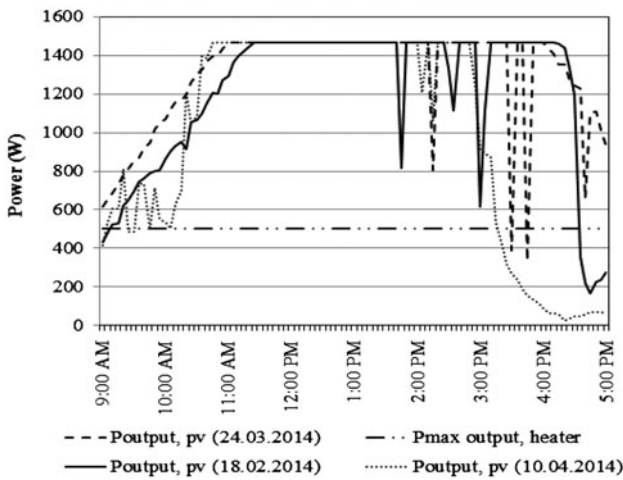


Fig. 6. Diurnal variations of output power of PV modules and maximum output power of heater used in CSSPVH during three typical days from 9 am to 5 pm.

($P_{output,heater}$) with the time interval of 5 min from 9 am to 5 pm are shown in Fig. 9. The rates of hourly and cumulative output power of PV-modules ($P_{h,pv}$ and $P_{c,pv}$) from 7 am to 7 pm are also presented in Table 6. It can be observed from Fig. 9 and Table 6 that the rate of hourly output power of PV-modules was always higher than the maximum output power of AC heater from 9 am to 5 pm, corresponding to the available solar radiation intensities in this period of time. Thus, the output power differences between PV-modules and AC heater were stored using

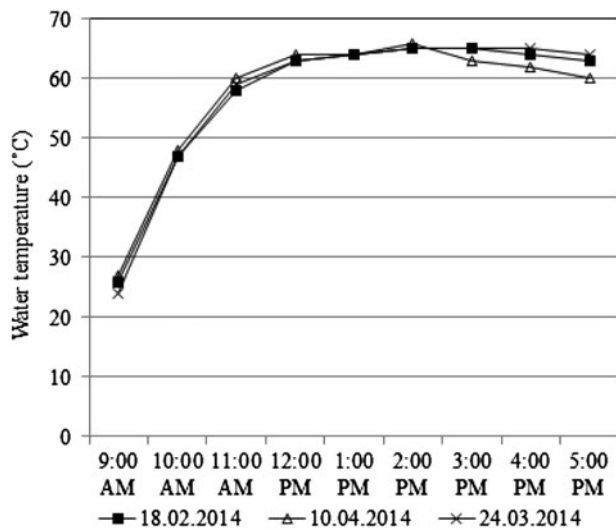


Fig. 7. Diurnal variations of water temperature for three typical days from 9 am to 5 pm using CSSPVH.

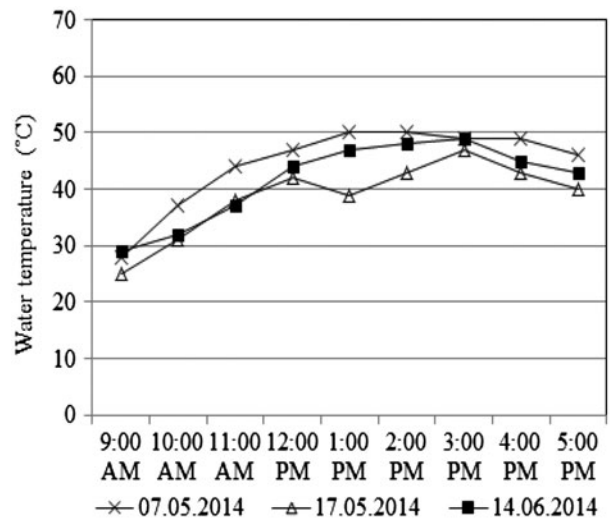


Fig. 8. Diurnal variations of water temperature for three typical days from 9 am to 5 pm using CSS.

4 × 150 Ah batteries in CSSPVH system to ensure 24 h operation of the still.

4.6. Expected time of the heater usage and expected productivity of CSSPVH

The values of V_{pmax} of four batteries were 2 × 24 V (Table 2) and the maximum current power of AC heater ($I_{pmax,heater}$) was 2.27 A, which was obtained by dividing the maximum power output of heater

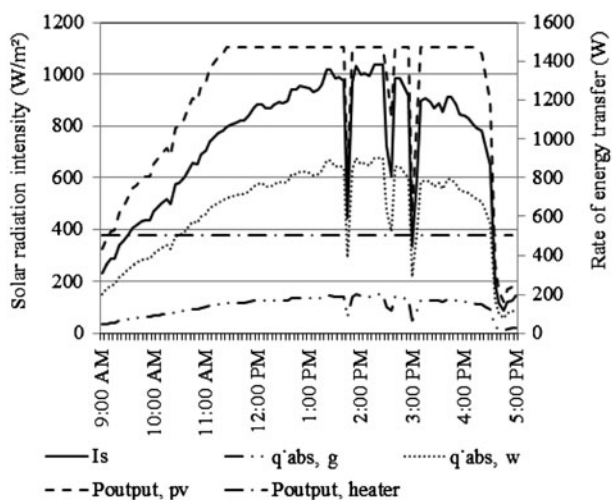


Fig. 9. Variations of solar radiation intensities vs. rate of energy transfers for CSSPVH from 9 am to 5 pm on 18 February 2014.

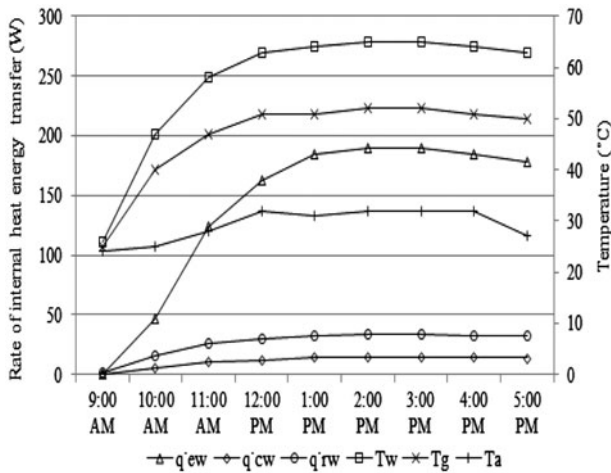


Fig. 10. Diurnal variations of T_w , T_g , and T_a vs. the rate of evaporative, convective, and radiative heat energy transfers of CSSPVH from 9 am to 5 pm on 18 February 2014.

($P_{max,heater}$) (500 W) by the maximum power voltage of heater ($V_{pmax,heater}$) (220 V) (Table 2).

Table 7 shows the hourly current power of four batteries ($I_{ph,batteries}$), expected time of AC heater usage (ET) and cumulative expected time of AC heater usage (CET), respectively, on 18 February 2014 from 7 am to 7 pm. The hourly current power of four batteries ($I_{ph,batteries}$) was obtained by dividing the hourly power output of six PV modules ($P_{h,pv}$) by the maximum power voltage of the batteries ($V_{pmax,batteries}$). The expected time (ET) of AC heater usage in the solar still basin was determined by dividing the hourly current power of batteries ($I_{ph,batteries}$) by the maximum current power of heater ($I_{pmax,heater}$) (Table 7). It was

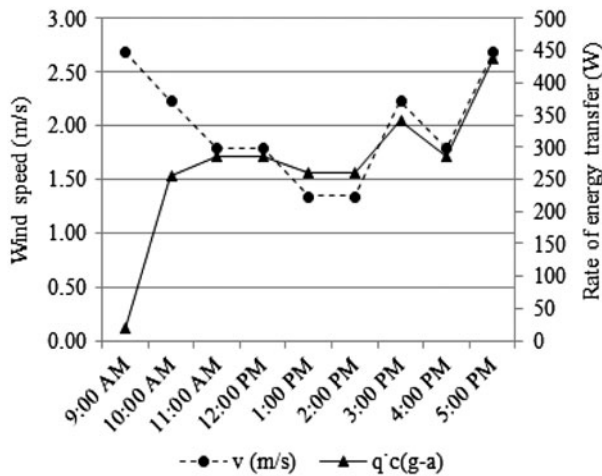


Fig. 11. Variations of wind speed and heat energy losses of CSSPVH from 9 am to 5 pm on 18 February 2014.

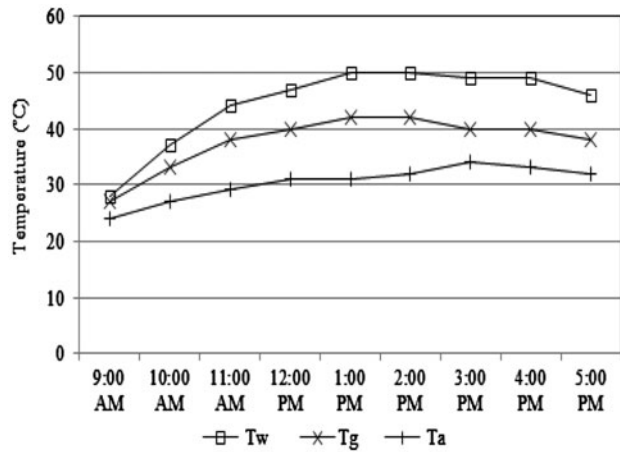


Fig. 12. Variations of T_w , T_g of CSS and T_a from 9 am to 5 pm on 07 May 2014.

observed that ET increases with the increase in I_s and $P_{h,pv}$ (Figs. 6, 9 and Table 7). The CET of heater was found by accumulating the values of ET which was obtained as 97 h shown in Table 7. It shows the number of hours (97 h) that one AC heater can be used to heat the basin water. It was observed that by exposing the six pv modules to direct sun radiation during one day such as 18 February 2014, the expected cumulative time (CET) to use one AC heater with the P_{max} of 500 W can be prolonged to about 97 h due to the powering of the heater by the four batteries as power sources.

The amount of water produced experimentally by CSSPVH for 8 h (M_{cexp}) is about 5.3 kg/m² from 9 am to 5 pm (Fig. 13) on 18 February 2014, making the average hourly experimental output of CSSPVH to be

Table 7
Expected time of usage of one AC heater^a

Time	$I_{ph,batteries}$ (Ah)	ET (h)	CET (h)
7 am–8 am	0.212	–	–
8 am–9 am	5.05	2	2
9 am–10 am	13.6	6	8
10 am–11 am	21.9	9	17
11 am–12 pm	29.88	13	30
12 pm–1 pm	30.62	13	43
1 pm–2 pm	29.48	13	56
2 pm–3 pm	29.76	13	69
3 pm–4 pm	28.52	12	81
4 pm–5 pm	18.13	8	89
5 pm–6 pm	12.73	5	94
6 pm–7 pm	8.22	3	97

Notes: CET: cumulative expected time of AC heater usage; ET: expected time of AC heater usage.

^a $I_{ph,batteries}$: the hourly current power of four batteries.

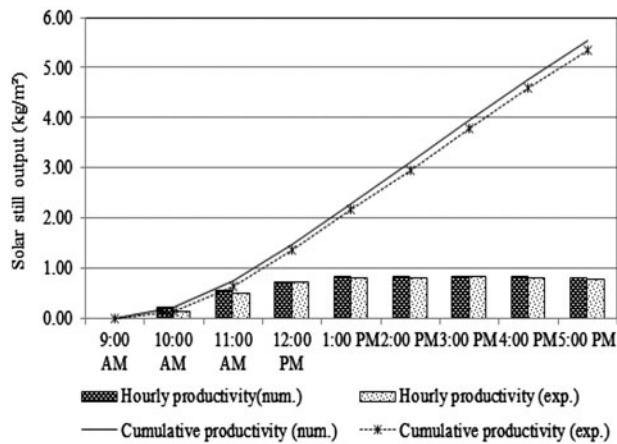


Fig. 13. Experimental and numerical productivity of CSSPVH from 9 am to 5 pm on 18 February 2014.

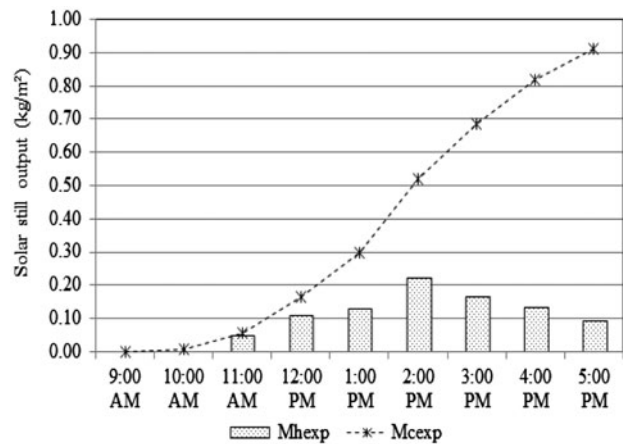


Fig. 14. Variations of M_{hexp} and M_{cexp} for CSS from 9 am to 5 pm on 07 May 2014.

0.7 kg/m². Therefore, the productivity of one CSSPVH using one 500 W AC for 24 h is expected to be up to 16 kg/m² for 24 h as shown in Fig. 17 because the CET of the heater usage is 97 h (Table 7). This research shows higher productivity as compared to the other active solar still studies in India [3,4,9,17,21], Oman [5,6], Peru [7], Saudi Arabia [8], Malaysia [22–24], Jordan [25,26], Iran [27,28], and Egypt [29]. A comparison of the daily output of CSSPVH with the outputs of some other active solar stills using separate additional heat storage collector is shown in Table 8. CSSPVH is may be more costly than the CSS and other mentioned active solar stills, but it is more effective and sustainable to operate the system for 24 h using CSSPVH rather than CSS due to more water production (Figs. 13 and 14) and to maintain the water production at high rates (Fig. 17) during night time as well as the sunshine hours. The number of heaters, which is four, can be obtained by dividing the CET of

heater (97 h) over the 24 h period. Therefore, to optimize the consumption of the stored power in four batteries, it is recommended to fabricate four similar size solar stills with the use of four AC heaters, each having 500 W power, in order to enhance the productivity. Since an AC heater has the capacity of producing 16 kg/m² of potable water for 24 h and the CET for heater usage is 97 h, therefore four AC heaters will be operational to produce about 64 kg/m² of water in 24 h.

Table 9 shows the analysis of error between the hourly experimental and numerical productivities for CSSPVH from 9 am to 5 pm on 18 February 2014. The Root Mean Squared Error (RMSE) of hourly experimental and numerical outputs of CSSPVH was low (0.0003) and the high correlation of 0.99736 with R^2 of 0.99472 showed the linear relationship between the hourly experimental (M_{hexp}) and numerical (M_{hn}) productivities.

Table 8
Performance of some active solar stills coupled with solar heat storage collectors

No.	Heat storage methods	Country	Maximum production rate (kg/m ² d)	Refs.
1	A single slope solar still connected to the two separate solar flat plate collectors	India	3.77	[3]
2	A single slope solar still coupled with 10 evacuated tubes collector	India	3.8	[4]
3	A single slope solar still connected to an inverted absorber	Oman	6.3	[5]
4	A solar still integrated with a parabolic-trough concentrator	Peru	6.36	[7]
5	A solar still integrated with photovoltaic modules, batteries and AC heater (CSSPVH)	Malaysia	16	This work

Table 9

Analysis of error (RMSE) between hourly experimental and numerical outputs from 9 am to 5 pm on 18 February 2014^a

Time	M_{hexp}	M_{hn}	Residual	Squared	RMSE	Correlation	Coefficient of determination (R^2)
9 am	0	0.00	0.00	0.0000	0.0003	0.99736	0.99472
10 am	0.14	0.20	-0.07	0.0043			
11 am	0.50	0.54	-0.05	0.0024			
12 pm	0.72	0.72	0.01	0.0001			
1 pm	0.80	0.81	-0.01	0.0002			
2 pm	0.80	0.84	-0.04	0.0013			
3 pm	0.82	0.84	-0.02	0.0003			
4 pm	0.81	0.81	0.00	0.0000			
5 pm	0.76	0.78	-0.02	0.0006			

Notes: Squared = Residual²; Residual = $M_{\text{hexp}} - M_{\text{hn}}$.

^aRMSE = SQRT (SUM (Squared values)/9).

Table 10

Quality of water from lake and distilled water from solar stills

Water quality parameter	Lake water (average)	Distilled water (average)	WHO standards [30,31]
pH	7.2	6.85	6.5–8.0
Total dissolved solids (mg/l)	650	22.50	<600
Nitrate (mg/l)	7.26	0.43	<50
Iron (mg/l)	18.20	0.06	<0.3
Turbidity (NTU)	38.45	0.98	<5
Color (Hazen unit)	7	0	<5

4.7. Water quality analysis

Table 10 shows the water quality parameters of the water produced from lake water together with the WHO standards for drinking water. The average values of pH, Total dissolved solids (TDS), nitrate,

iron, turbidity, and color reduced from 7.2, 650 mg/l, 7.26 mg/l, 18.20 mg/l, 38.45 NTU, and 7 Hazen unit before experiment to 6.85, 22.50 mg/l, 0.43 mg/l, 0.06 mg/l, 0.98 NTU, and 0 Hazen unit after experiment, respectively; which showed that water

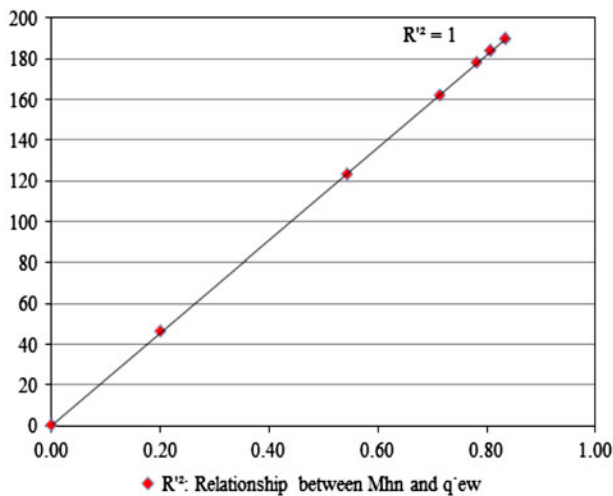


Fig. 15. Relationship between M_{hn} and the rate of \dot{q}_{ew} of CSSPVH from 9 am to 5 pm on 18 February 2014.

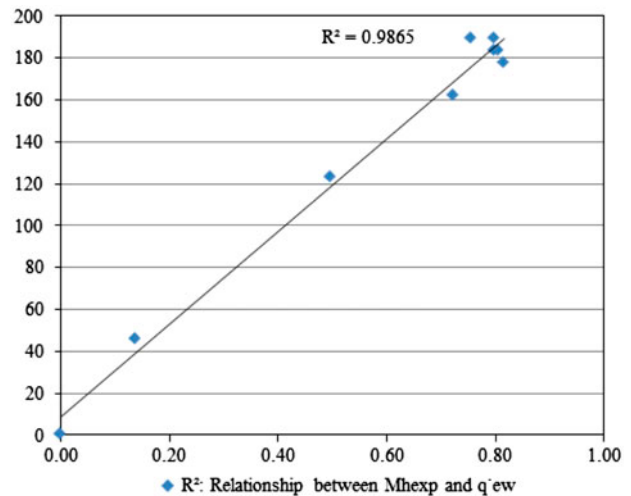


Fig. 16. Relationship between M_{hexp} and the rate of \dot{q}_{ew} of CSSPVH from 9 am to 5 pm on 18 February 2014.

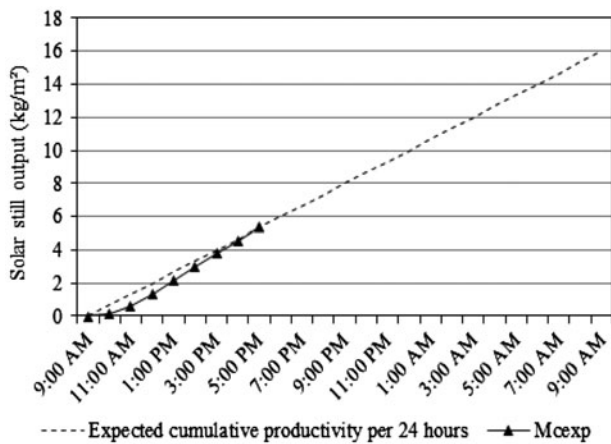


Fig. 17. Expected cumulative productivity with the use of one AC heater during 24 h and cumulative experimental output of CSSPVH per 8 h (M_{cexp}) from 9 am to 5 pm on 18 February 2014.

produced by the still is within the accepted range of WHO drinking water standards in this work [30,31].

5. Conclusions

Despite daily fluctuations due to cloud coverage, solar energy can be effectively harnessed, stored, and converted to electrical energy for clean water production using a double slope solar still equipped with 6×245 W PV modules, 4×150 Ah batteries and one 500 W AC heater. In this work, the conventional solar still (CSS) using direct sun radiation only produced 0.9, 0.6, and 0.6 kg/m² of clean water during three experimental days having different average solar intensities from 9 am to 5 pm, while the solar still equipped with a PV-AC heater system (CSSPVH) produced 5.3, 5.7, and 5.1 kg/m² during different three days under Malaysia's meteorological conditions. The integrated solar still used in this study produced about 6 to 10 times as much water as the conventional still. A numerical model of CSSPVH was simulated using mathematical equations of heat and mass transfer. The model showed that the numerical output is in good agreement with experimental productivities. The energy balance equations of condensing cover and basin water were also defined and developed. The CSSPVH system is a sustainable design due to the use of solar energy to heat basin water, and electricity production using photovoltaic modules and storing it using batteries to ensure 24 h operation of the system. Thus, the system has the potential of producing potable water for a long period of time with low maintenance cost, even in areas with very low daily solar radiation intensity. This design can also be

applied in arid, remote, rural, suburban, and coastal areas. The quality of the water produced was within the acceptable range of World Health Organization (WHO) drinking water standards.

Acknowledgment

The authors are grateful to the Universiti Teknologi PETRONAS management, research and innovation office (UTPRIO) for providing fund (Project code: STIRF NO. 0153AA-C55) for this research.

Nomenclature

M_{hn}	—	hourly numerical condensed water production rate per unit area (kg/m ²)
m_{fw}	—	mass of feed water (kg)
m_{bd}	—	mass of distilled water from basin water (kg)
E_g	—	energy transfer of condensing glass cover (W)
$\dot{q}_{abs,g}$	—	rate of heat energy absorption by condensing glass cover due to solar radiation intensity (W)
\dot{q}_{ew}	—	rate of convective heat energy transfer from water surface to the inner glass cover (W)
\dot{q}_{ew}	—	rate of evaporative heat energy transfer from water surface to the inner glass cover (W)
\dot{q}_{rw}	—	rate of radiative heat energy transfer from water surface to the inner glass cover (W)
$\dot{q}_{c(g-a)}$	—	rate of convective heat losses from outer glass cover to ambient air (W)
$\dot{q}_{r(g-a)}$	—	rate of radiative heat losses from outer glass cover to ambient air (W)
$\dot{q}_{ref(g-a)}$	—	rate of reflective heat energy transfer from outer glass cover to ambient air (W)
m_g	—	mass of glass cover (kg)
C_g	—	specific heat capacity of glass cover (J/kg °C)
T_g	—	temperature of inner glass cover (°C)
t	—	time (hour)
$E_{w,b}$	—	energy transfer of basin and water (W)
$\dot{q}_{abs,w}$	—	rate of heat energy absorption of basin water due to passing solar radiation intensity through the glass cover (W)
\dot{q}_h	—	rate of heat energy transfer from AC heater to the basin water (W)
$\dot{q}_{ref(w,b)}$	—	rate of reflective heat energy transfer from water to inner surface of glass cover (W)
\dot{q}_d	—	rate of heat losses from distilled water to the ambient air (W)
m_w	—	mass of water in basin (kg)
C_w	—	specific heat capacity of water (J/kg °C)
m_b	—	mass of basin (kg)

C_b	— specific heat capacity of basin (J/kg °C)
L	— latent heat of water evaporation (J/kg)
h_{cw}	— convective heat transfer coefficient from water to condensing cover (W/m ² °C)
h_{rw}	— radiative heat transfer coefficient from water to condensing cover (W/m ² °C)
h_{ew}	— evaporative heat transfer coefficient from water to condensing cover (W/m ² °C)
A_b	— area of basin (m ²)
T_w	— temperature of water in basin (°C)
P_w	— saturated vapor pressure at water surface (N/m ²)
P_g	— saturated vapor pressure at condensing glass surface (N/m ²)
$A_{g,E}$	— area of glass cover exposed to east side of sun radiation (m ²)
I_E	— solar radiation intensity passing through the east side of the glass cover (W/m ²)
$A_{g,W}$	— area of glass cover exposed to west side of sun radiation (m ²)
I_W	— solar radiation intensity passing through the west side of the glass cover (W/m ²)
$P_{\text{output,pv}}$	— output power of pv modules (W)
PV	— photovoltaic modules
n	— number of photovoltaic modules
η_{pv}	— efficiency of pv modules (%)
A_{pv}	— area of pv modules (m ²)
I_S	— solar radiation intensity (W/m ²)
$h_{c(g-a)}$	— convective heat transfer coefficient from glass cover to ambient air (W)
V	— wind speed (m/s)
m_d	— mass of distilled water (kg)
T_a	— temperature of ambient air (°C)
M_{hexp}	— hourly experimental condensed water production rate per unit area (kg/m ²)
M_{cn}	— cumulative numerical productivity (kg/m ²)
M_{cexp}	— cumulative experimental productivity (kg/m ²)
ϵ_{eff}	— effective emissivity derived from water and glass cover emissivity
σ	— Stefan's constant, 5.6×10^{-8} W/m ² K ⁴
ϵ_g	— glass cover emissivity
ϵ_w	— basin water emissivity
τ_g	— transmissivity of condensing glass cover
α_g	— absorptivity of glass cover

References

- [1] A. Ahsan, M. Imteaz, U.A. Thomas, M. Azmi, A. Rahman, N.N. Nik Daud, Parameters affecting the performance of a low cost solar still, *Appl. Energy* 114 (2014) 924–930.
- [2] S. Jasrotia, A. Kansal, V.V.N. Kishore, Application of solar energy for water supply and sanitation in Arsenic affected rural areas: A study for Kaudikasa village, India, *J. Clean. Prod.* 37 (2012) 389–393.
- [3] G. Singh, S. Kumar, G.N. Tiwari, Design, fabrication and performance evaluation of a hybrid photovoltaic thermal (PVT) double slope active solar still, *Desalination* 277 (2011) 399–406.
- [4] R.V. Singh, S. Kumar, M.M. Hasan, M.E. Khan, G.N. Tiwari, Performance of a solar still integrated with evacuated tube collector in natural mode, *Desalination* 318 (2013) 25–33.
- [5] R. Dev, S.A. Abdul-Wahab, G.N. Tiwari, Performance study of the inverted absorber solar still with water depth and total dissolved solid, *Appl. Energy* 88 (2011) 252–264.
- [6] G.N. Tiwari, S. Suneja, Performance evaluation of an inverted absorber solar still, *Energy Convers. Manage.* 39 (1998) 173–180.
- [7] E. Sættone, Desalination using a parabolic-trough concentrator, *Appl. Solar Energy* 48 (2012) 254–259.
- [8] A.Z. Al-Garni, Productivity enhancement of solar still using water heater and cooling fan, *J. Sol. Energy Eng.* 134 (2012) 031006.
- [9] G.N. Tiwari, V. Dimri, A. Chel, Parametric study of an active and passive solar distillation system: Energy and exergy analysis, *Desalination* 242 (2009) 1–18.
- [10] A. El-Bahi, D. Inan, A solar still with minimum inclination, coupled to an outside condenser, *Desalination* 123 (1999) 79–83.
- [11] B.A. Akash, M.S. Mohsen, W. Nayfeh, Experimental study of the basin type solar still under local climate conditions, *Energy Convers. Manage.* 41 (2000) 883–890.
- [12] G.N. Tiwari, Madhuri, Effect of water depth on daily yield of the still, *Desalination* 61 (1987) 67–75.
- [13] S.M.A. Moustafa, G.H. Brusewitz, D.M. Farmer, Direct use of solar energy for water desalination, *Sol. Energy* 22 (1979) 141–148.
- [14] I. Al-Hayeka, O.O. Badran, The effect of using different designs of solar stills on water distillation, *Desalination* 169 (2004) 121–127.
- [15] M.A.S. Malik, G.N. Tiwari, A. Kumar, M.S. Sodha, *Solar Distillation*, Pergamon Press, Oxford, 1982.
- [16] R.V. Dunkle, Solar water distillation: The roof type still and a multiple effect diffusion still, *ASME Proceedings of International Heat Transfer*, Part V, University of Colorado, Boulder, CO, 1961.
- [17] S. Toure, P. Meukam, A numerical model and experimental investigation for a solar still in climatic conditions in Abidjan (Côte d'Ivoire), *Renewable Energy* 11 (1997) 319–330.
- [18] K.K. Murugavel, S. Sivakumar, J.R. Ahmed, K.K.S.K. Chockalingam, K. Srithar, Single basin double slope solar still with minimum basin depth and energy storing materials, *Appl. Energy* 87 (2010) 514–523.
- [19] M. Herrando, C.N. Markides, K. Hellgardt, A UK-based assessment of hybrid PV and solar-thermal systems for domestic heating and power: System performance, *Appl. Energy* 122 (2014) 288–309.
- [20] J.H. Watmuff, W.W.S. Charters, D. Proctor, Solar and wind induced external coefficients solar collectors, *Int. Revue d' Helio-technique*, 2nd Quarter, (1977) p. 56.
- [21] A. Kumar, M. Singh, J.D. Anand, Transient performance of a double-basin solar still integrated with a heat exchanger, *Energy* 14 (1989) 643–652.

- [22] A. Riahi, K.W. Yusof, N.B. Sapari, B.S.M. Singh, A.M. Hashim, Novel configurations of solar distillation system for potable water production, *IOP Conf. Ser. Earth Environmen. Sci.* 16 (2013) 012135, doi: [10.1088/1755-1315/16/1/012135](https://doi.org/10.1088/1755-1315/16/1/012135).
- [23] A. Riahi, K.W. Yusof, N.B. Sapari, A. Malakahmad, A.M. Hashim, B.S.M. Singh, Potable water production by using triangular solar distillation systems in Malaysia, in: *Proceeding of IEEE Conference on Clean Energy and Technology (CEAT), Langkawi, 2013*, pp. 473–477, doi: [10.1109/CEAT.2013.6775679](https://doi.org/10.1109/CEAT.2013.6775679).
- [24] A. Riahi, K.W. Yusof, M.H. Isa, B.S.M. Singh, A. Malakahmad, N.B. Sapari, Experimental investigation on the performance of four types of solar stills in Malaysia, *Appl. Mech. Mater.* 567 (2014) 56–61.
- [25] Y. Taamneh, M.M. Taamneh, Performance of pyramid-shaped solar still: Experimental study, *Desalination* 291 (2012) 65–68.
- [26] M. Abu-Qudais, B.A.K. Abu-Hijleh, O.N. Othman, Experimental study and numerical simulation of a solar still using an external condenser, *Energy* 21 (1996) 851–855.
- [27] J.A. Esfahani, N. Rahbar, M. Lavvaf, Utilization of thermoelectric cooling in a portable active solar still—An experimental study on winter days, *Desalination* 269 (2011) 198–205.
- [28] N. Rahbar, J.A. Esfahani, Experimental study of a novel portable solar still by utilizing the heatpipe and thermoelectric module, *Desalination* 284 (2012) 55–61.
- [29] Z.S. Abdel-Rehim, A. Lasheen, Improving the performance of solar desalination systems, *Renewable Energy* 30 (2005) 1955–1971.
- [30] World Health Organization, Guidelines for drinking - water quality (electronic resource): Incorporating the first and second Addenda, recommendations, third ed., vol. 1, 2008, Geneva, Accessed at: http://www.who.int/water_sanitation_health/dwq/fulltext.pdf on 15 May 2011.
- [31] World Health Organization, Guidelines for drinking-water quality, fourth ed., (2011), Geneva, Accessed at: http://whqlibdoc.who.int/publications/2011/9789241548151_eng.pdf?ua=1 on 10 March 2015.